Electronic Supplementary Information

Cluster-derived TiO_2 nanocrystals with multiple carbon coupling for interfacial pseudo-capacitive lithium storage

Xi Bi,[a, c, +] Zhanli Chai,[c, +] Yongjian Niu,[a] Yangyang Feng,[b] Linlin Zhang,[a, b *] and Cheng Wang[a]

[a] Tianjin Key Laboratory of Advanced Functional Porous Materials and Center for Electron Microscopy, Institute for New Energy Materials & Low-Carbon Technologies, School of Materials Science and Engineering, Tianjin University of Technology, Tianjin 300384, China

[b] CAS Key Laboratory of Design and Assembly of Functional Nanostructures, Fujian Key Laboratory of Nanomaterials, Fujian Institute of Research on the Structure of Matter, Chinese Academy of Sciences, Fuzhou 350002, China

[c] Inner Mongolia Key Laboratory of Chemistry and Physics of Rare Earth Materials, School of Chemistry and Chemical Engineering, Inner Mongolia University, Hohhot 010021, China

[+] These authors contributed equally to this work.

* Corresponing author: Linlin Zhang; Email: zhanglinlin_cn@126.com

Table of Content

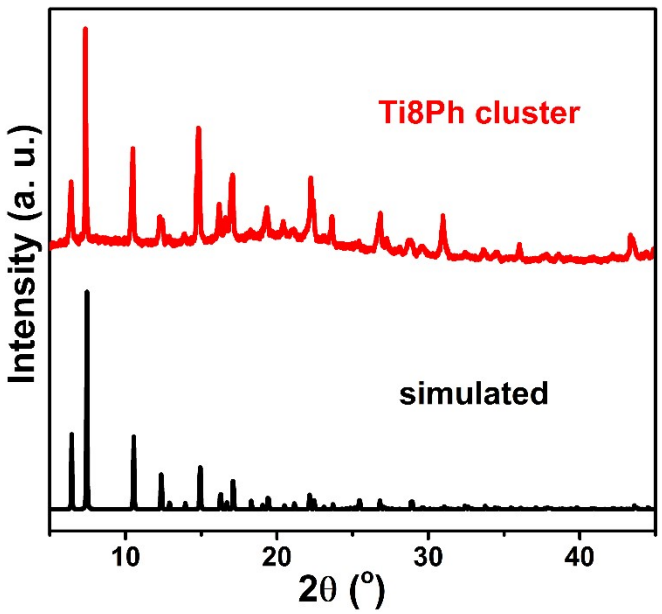

Figure S1 XRD patterns of the as-synthesized Ti8Ph cluster and the simulated ones.

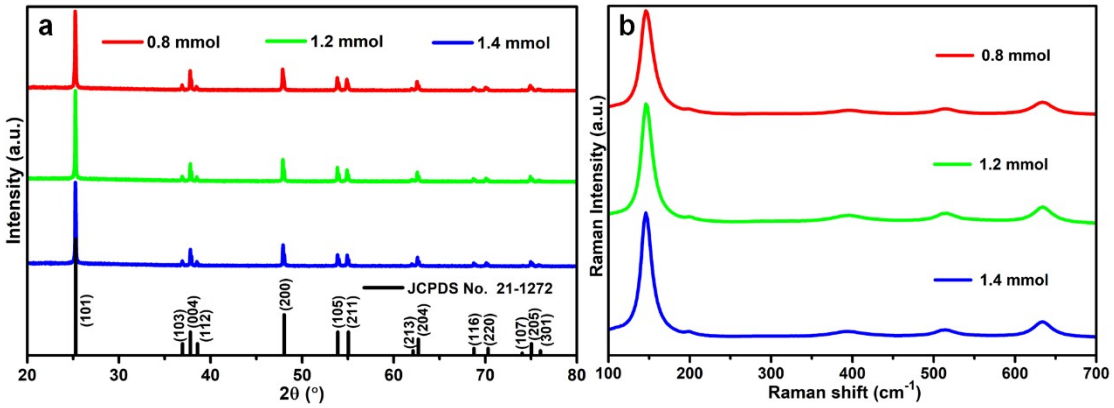

Figure S2 XRD patterns (a) and Raman spectra (b) of the three typical samples obtained with 2 ml of DMF and 8 ml of H_2O using 0.8 mmol, 1.2 mmol and 1.4 mmol of NaF using Ti_8Ph as the precursor.

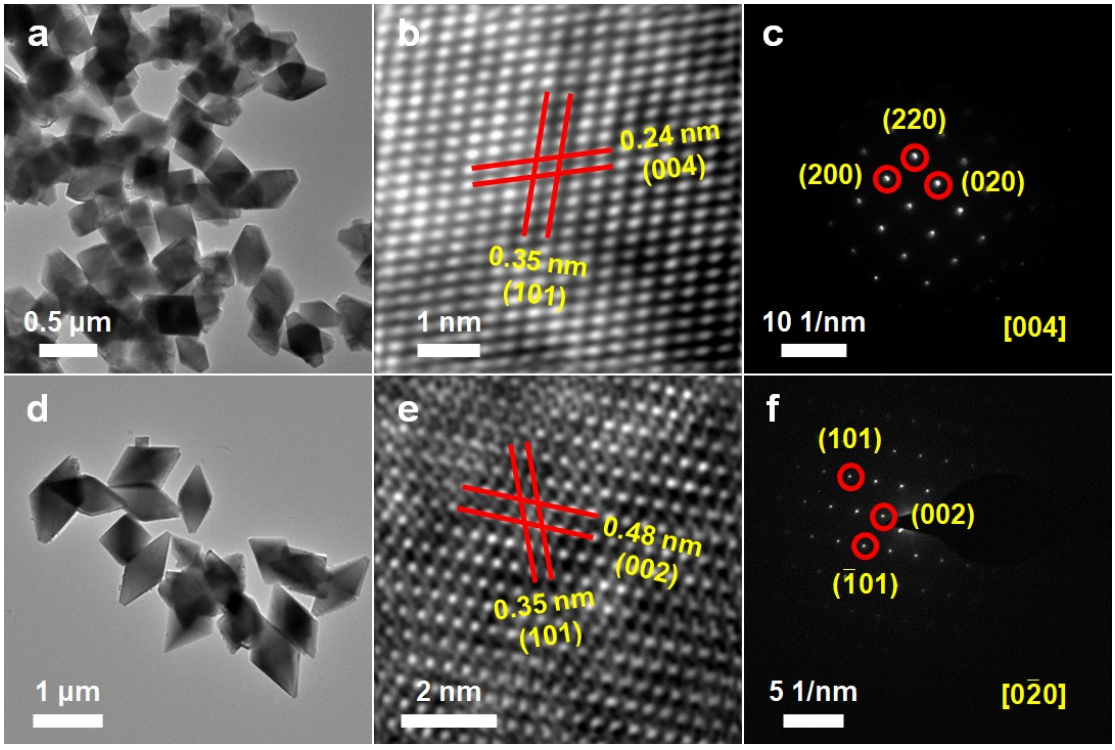

Figure S3 TEM (a,d), HRTEM (b, e) images and SAED patterns (c, f) of the samples obtained with 2 ml of DMF and 8 ml of H_2O using 0.8 mmol (a-c) and 1.4 mmol (d-f) of NaF using Ti_8Ph as the precursor.

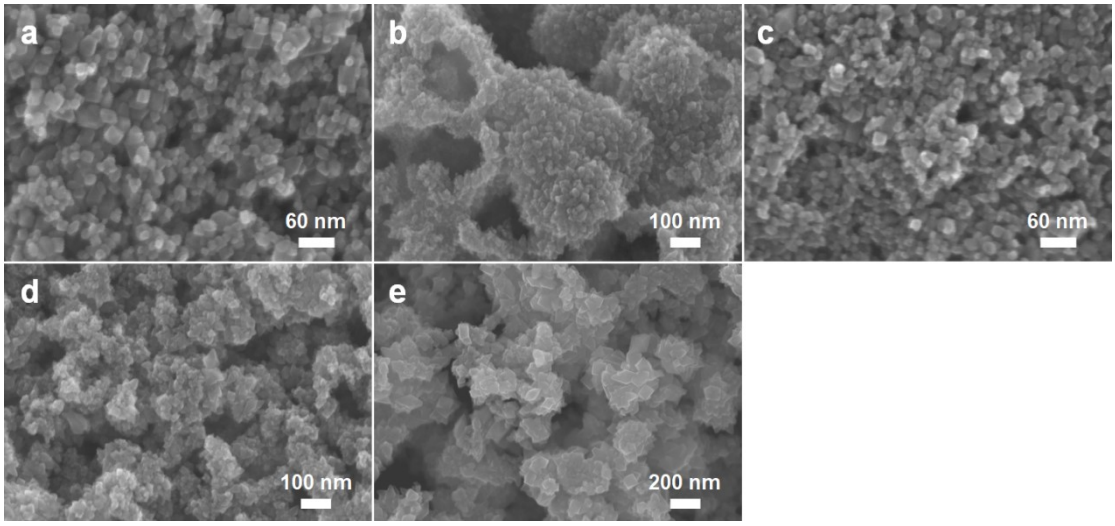

Figure S4 SEM images of products obtained with 10 ml H_2O and different amounts of NaF. (a) 0.4 mmol, (b) 0.8 mmol, (c)1.2 mmol, (d)1.6 mmol, (e) 2.0 mmol.

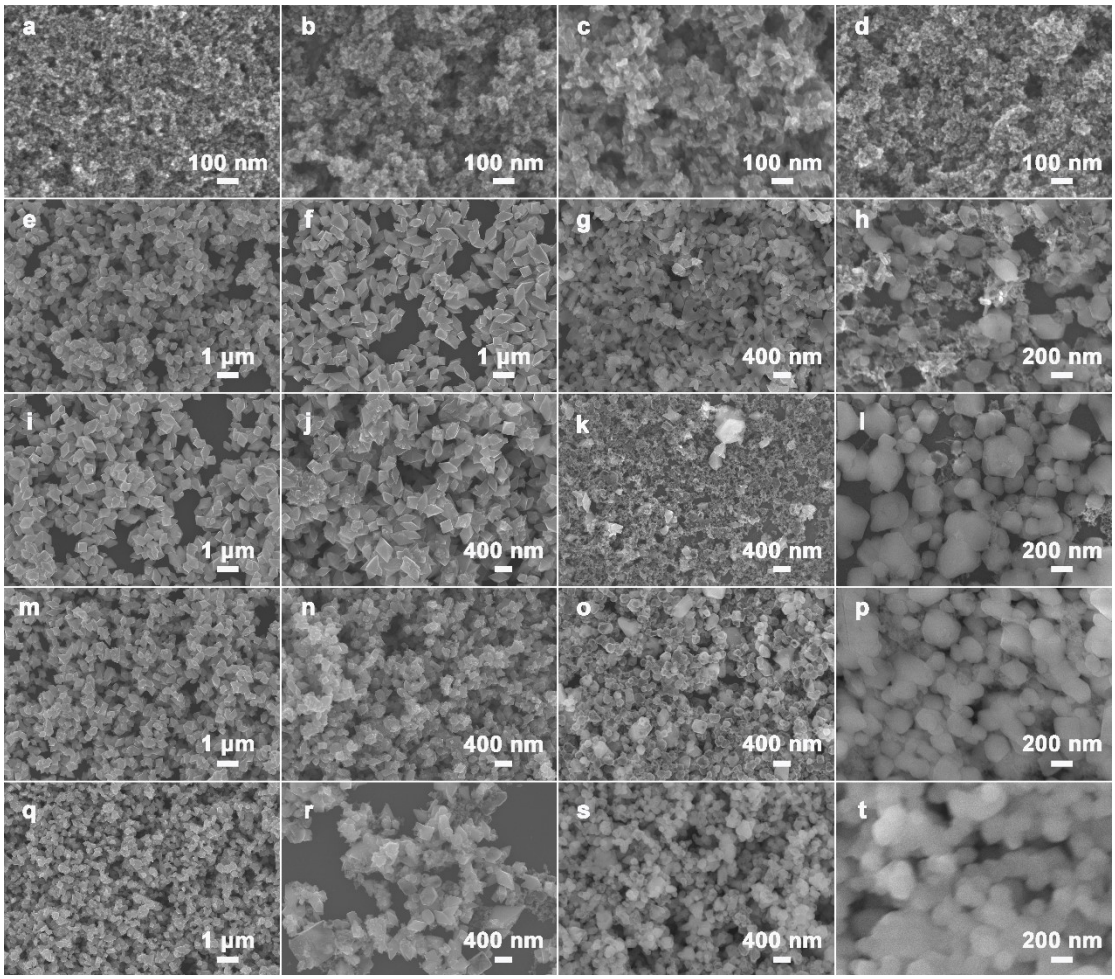

Figure S5 SEM images of products obtained with *x* ml of DMF, *y* ml of H_2O and *z* mmol of NaF. (a, e, I, m, q) *x*=2, *y*=8, (b, f, j, n, r) *x*=4, *y*=6, (c, g, k, o, s) *x*=6, *y*=4, (d, h, l, p, t) *x*=8, *y*=2; (a-d) *z*=0.4, (e-h) *z*=0.8, (i-l) *z*=1.2, (m-p) *z*=1.6, (q-t) *z*=2.0.

To scrutinize the influences of H_2O, DMF and NaF on the products, a series of control experiments were conducted. With exclusive DMF, only sol-like species could be obtained. With H_2O as the sole solvent, only small irregular nanoparticles could be observed (**Figure S4**). With mixed solvent of DMF and H_2O, well-defined truncated tetragonal bipyramids gradually showed up and grew bigger and sharper with increasing dosage of NaF (**Figure S5**). As the ratio of H_2O increased, less NaF was needed to convert Ti_8Ph into faceted TiO_2 nanocrystals. However, in the presence of insufficient and excessive NaF, small irregular nanoparticles and aggregated species other than TiO_2 were produced, respectively, regardless of the solvent composition. Hence, appropriate amount of DMF, H_2O and NaF was essential to form uniform and well-faceted TiO_2 nanocrystals. Since DMF could well dissolve Ti_8Ph, the cluster probably existed in the form of molecules in the reaction solution. It could serve either as building blocks to directly participate in the construction of nanocrystals, or as reservoirs that were able to continuously and steadily release Ti ions during the reaction. Such bottom-up synthetic processes may be accounted for the homogeneous nucleation and the resulting uniform generation of TiO_2. H_2O, another solvent, acted as both the source and medium for the subsequent hydrolysis and condensation of the Ti-O cluster. As is well-established, fluoride ions and HF are effective in promoting the exposure of (001) facets of anatase TiO_2 by tightly adsorbing on the (001) facets. Herein, NaF also played vital roles in facilitating the oriented growth of faceted TiO_2 nanocrystals. Yet to our surprise, the percentage of (001) facets gradually decreased with the increase of the amount of NaF. This unusual phenomenon might be rationalized by the large electronegativity of fluorine, which enabled fluoride ions to form hydrogen bonds with both H_2O and the aldehyde group of DMF. Besides, because of the electrostatic interaction, sodium ions would be attracted to the carboxylic acids surrounding the core of Ti_8Ph, and meanwhile the majority of fluoride ions would stay close to the sodium ions. As a result, the number of fluoride ions capable of adsorbing on the surfaces of TiO_2, particularly (001) facets, would be greatly declined, leading to less inhibited growth of the nanocrystals and gradual elimination of (001) facets. Therefore, it was reasonable to conclude that NaF was of paramount importance to the shape and size control of the TiO_2 nanocrystals. Its cooperative work with the precursor and solvents was also responsible for the oriented growth of the well-defined truncated tetragonal bipyramids of anatase TiO_2.

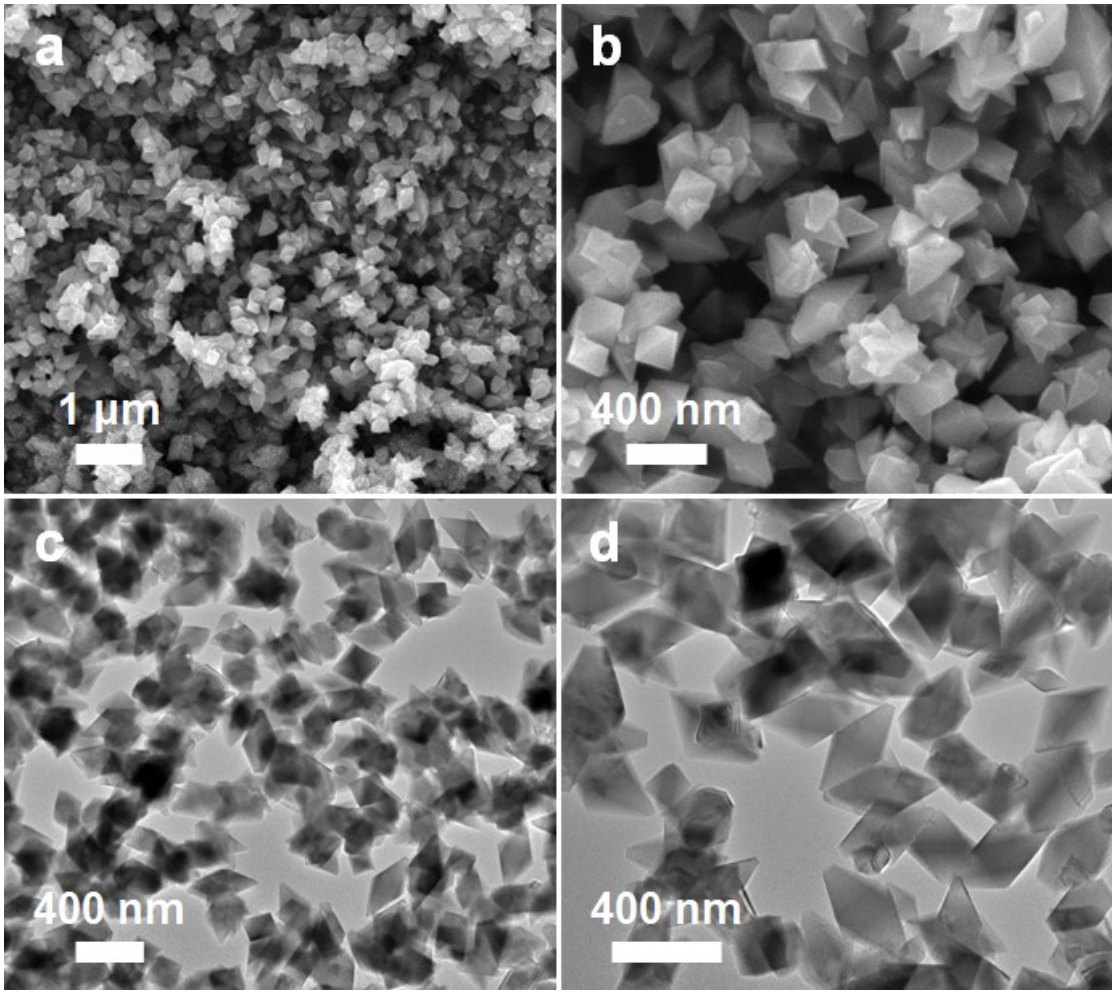

Figure S6 SEM and TEM images of pristine TiO_2 nanocrystals with the middle size.

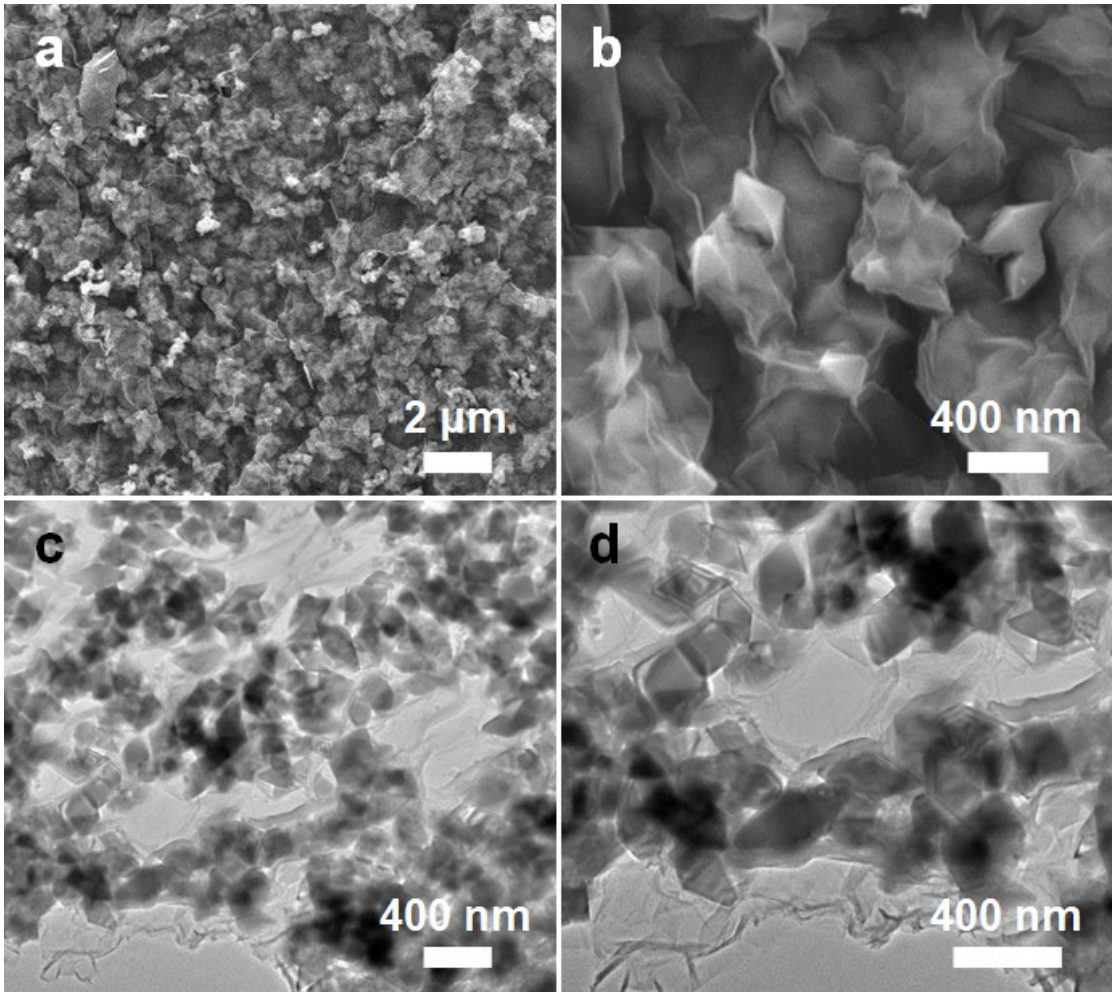

Figure S7 SEM and TEM images of TiO_2-rGO, in which TiO_2 nanocrystals were of the middle size.

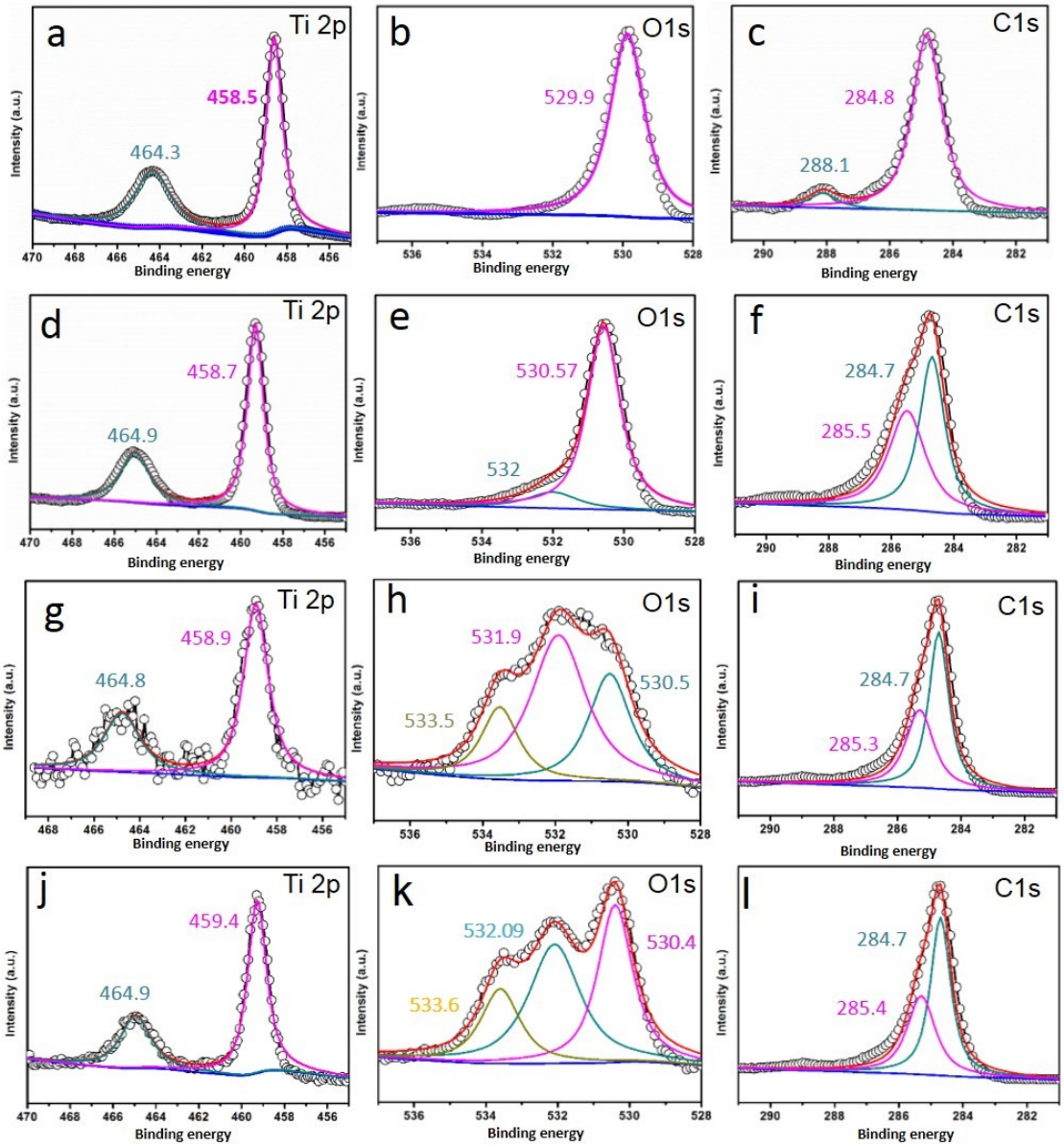

Figure S8 Ti 2p (a, d, g, j), O 1s (b, e, h, k) and C 1s (c, f, i, l) XPS of the four typical samples of TiO_2 (a-c), TiO_2-C (d-f), TiO_2-rGO (g-i), TiO_2-C-GO (j-l), in which TiO_2 nanocrystals were of the same middle size.

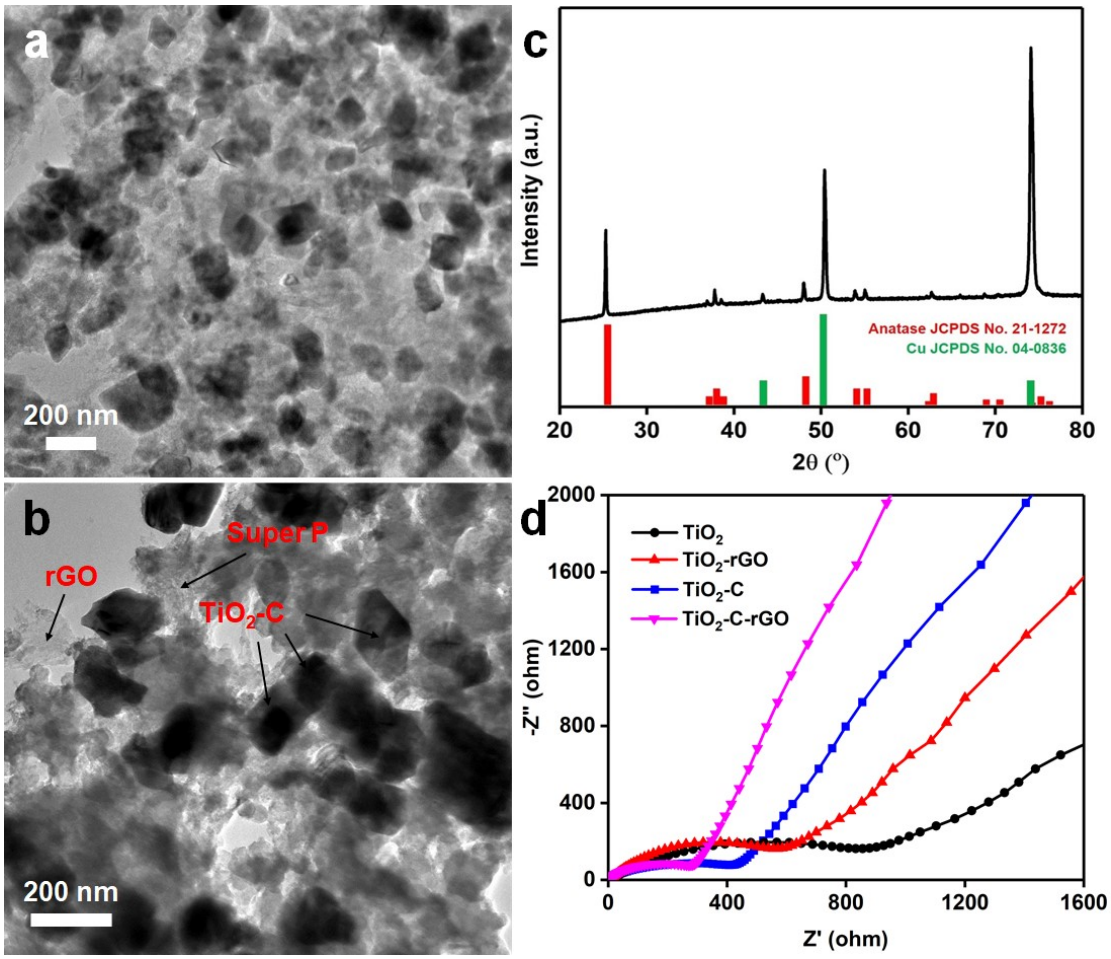

Figure S9 Characterizations of the active materials corresponding to TiO_2-C-rGO after cycling for more than 300 cycles at the current rate of 0.1 A g^{-1}. (a-b) TEM images (peeled off the copper foils), (c) XRD patterns (loaded on the copper foils), (d) Nyquist plots recorded at the open circuit voltage in the frequency range from 100 kHz to 100 mHz with an amplitude of 5 mV. For comparison, the corresponding Nyquist plots of TiO_2-C, TiO_2- rGO, and TiO_2 were also provided.

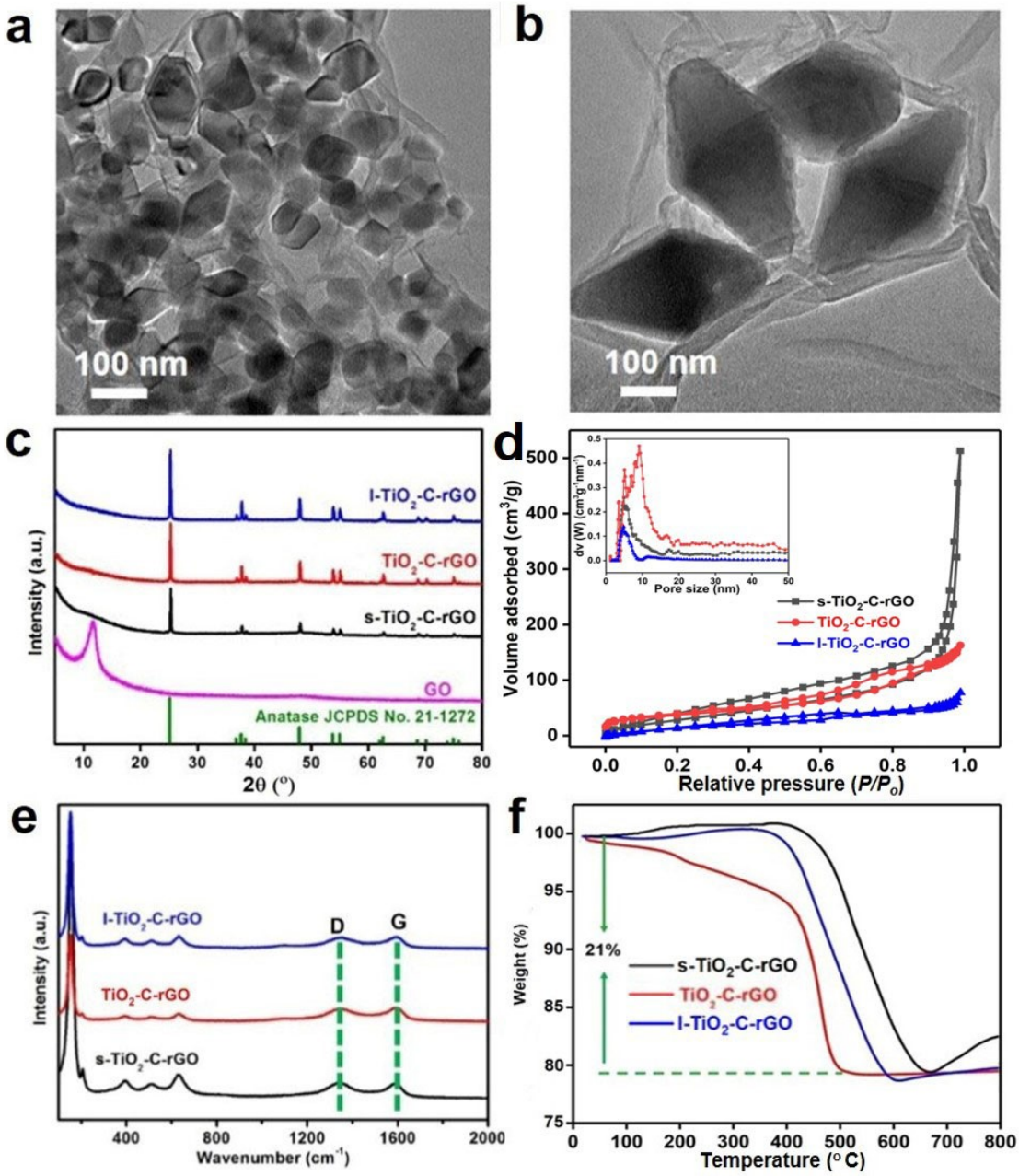

Figure S10 TEM images (a, s-TiO_2-C-rGO; b, l-TiO_2-C-rGO), XRD patterns (c), N_2 adsorption-desorption isotherms (d), Raman spectra (e), and TG curves (f) of s-TiO_2-C-rGO and l-TiO_2-C-rGO. For comparison, the latter four characterizations of TiO_2-C-rGO were also provided.

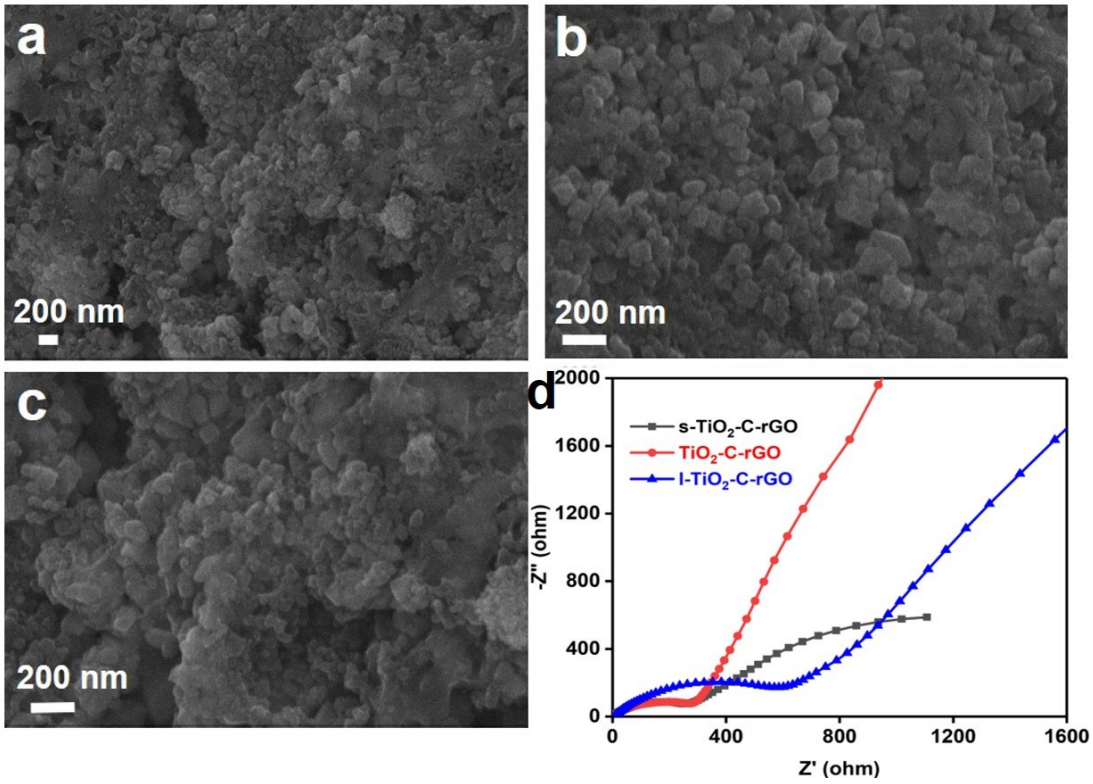

Figure S11 SEM images (a-c) and Nyquist plots (d) of the three composites of s-TiO_2-C-rGO (a), TiO_2-C-rGO (b) and l-TiO_2-C-rGO (c) after cycling for more than 300 cycles at the current rate of 0.1 A g^{-1}. The Nyquist plots were recorded at the open circuit voltage in the frequency range from 100 kHz to 100 mHz with an amplitude of 5 mV

Table S1 Comparisons of lithium storage performances with reported TiO_2-based nanostructures.

Materials	Initial capacity (mA h g^{-1}/A g^{-1})	Rate capacity (mA h g^{-1}/A g^{-1})	Long-term capacity (mA h g^{-1}/A g^{-1}/cycle)	Ref.
TiO_2-C-rGO	1797.6/0.1	714.3/0.5 563.7/1.0 446.2/2.0 337.6/5.0 211.4/10.0	398/5.0/600 834/0.1/300	This work
TiO_2-C	536.7/0.1	253.6/0.5 195.9/1.0 155.9/2.0 111.6/5.0 65.1/10.0	146.9/5.0/600 290.3/0.1/300	This work
TiO_2-rGO	522.4/0.1	189.2/0.5 144.9/1.0 116.1/2.0 87.3/5.0 51.9/10.0	57.2/5.0/600 240.5/0.1/300	This work
TiO_2	195.9/0.1	129.4/0.5 93.9/1.0 78.4/2.0 62.9/5.0 43.1/10.0	38.9/5.0/600 85.4/0.1/300	This work
Hierarchically assembled carbon-coated TiO_2	-	225/0.168 188/0.84 162/1.68 91/8.4	-	1
$TiO_{2-x}C_x$ decahedral plate	150/0.034	79/2.52	145/0.168/100	2
Porous TiO_2 nanofibers decorated with N-doped carbon	567/0.0335	354/0.1675 313/0.335 254/0.8375 204/1.675 156/3.35 97/6.7	368/0.08375/200 176/3.35/2000	3
Mesoporous TiO_2@N-doped Carbon	219/0.084	174/0.168 169/0.336 148/0.84 127/1.68 118/3.36	117/1.68/2000	4
TiO_2@carbon core-shell nanosheets	1098/0.23	388/0.12 294/0.23 247/0.46 198/1.2 172/2.3 147/4.6	549/0.23/300 385/4.6/2000	5
Ultrathin mesoporous TiO_2/flexible graphitized carbon	260/3.4	180/6.8 150/10.2	213/3.4/1000	6
TiO_2/nitrogen-doped carbon foams	259/0.1	188/0.2 169/0.5 147/1.0 104/2.0	149/1.0/100	7
Mesoporous TiO_2/carbon	909.4/0.1	441.0/0.1 413.7/0.2 345.5/0.5 289.7/1.0 237.8/2.0 206.8/3.0	270.1/1.0/500	8
Hierarchical TiO_2/C	283/0.084	159/0.168 128/0.336 103/0.84	188/0.084/200	9
TiO_2 hollow spheres with conformal carbon coating	225/0.1	177/0.2 164/0.5 151/1.0 131/2.0 114/5.0 91/10.0	178/0.1/100 137/1.0/1000	10
Mesoporous TiO_2 microfibers@N-doped carbon	347.2/0.085	200.0/0.17 181.5/0.34 152.6/0.85 124.6/1.7 78.0/5.1 60.0/8.5	150.0/0.85/100 127.2/1.7/100	11
Hierarchically porous TiO_2/graphitic carbon microspheres	189/0.084	123/0.84	138.5/0.084/50	12
TiO_2(B)@PGNS	864.9/0.1	373/0.1 335/0.2 297/0.5 274/1.0 232/2.0 199/5.0	573/1.0/600	13
TiO_{2-x}/GQD	360.5/0.84 425.1/0.168	144.6/2.52	160.1/1.68/500	14
TiO_2-rGO hollow spheres	265/0.0188	216/0.094 188/0.188 166/0.374 151/0.94 132/1.88 109/3.74	174.4/0.188/200 146/0.940/200	15
TiO_2-RGO	816/0.06	232/1.2	210/1.2/1000	16
Mesoporous TiO_2/graphene/mesoporous TiO_2 sandwich-like nanosheets	362/0.02	238/0.04 225/0.1 210/0.2 187/0.5 175/1.0	237/0.02/100	17
Graphene@mTiO_2@carbon nanosheets	195/0.2	-	110/0.2/100	18
TiO_2/GAs	605/0.1	99/5.0	200/0.1/50	19
Anatase TiO_2 quantum-dot/graphene nanosheet	272/0.168	161/0.336 145/1.68 101/8.4	191/1.68/100	20
Ultrafine TiO_2 nanoparticles/N-doped graphene foams	226/0.0168	190/0.0336 121/1.68 96/3.36	165/0.168/200 143/0.84/200	21
Ultrathin anatase TiO_2 nanosheet/rGO	256.4/0.0335	202/0.1675 183/0.335 157/0.8375 118/1.675 88.3/3.35	174.2/0.1675/200 112.9/1.675/260	22
TiO_2 nanocrystals/RGO sheets	352/0.1	94/10.0	-	23
Flower-like TiO_2/graphene	280/16.8	-	180/0.17/70	24
Double-shelled anatase/TiO_2(B) hollow microspheres	356.3/0.335	148.0/6.70	215.4/0.335/100 141.6/3.35/1000 125.7/6.70/1000	25
Hollow TiO_2 nanostructures	330/0.1	196/1.0 136/5.0	228/0.1/100 224/0.2/100 195/0.1/500	26
Mesoporous yolk–shell anatase TiO_2/TiO_2(B) microspheres	330/0.0336	181.8/6.72	260.1/0.168/500	27
TiO_2 spheres	216.9/0.084	189.1/0.168 167/0.336 136.4/0.84 101.7/1.68	169/0.168/100	28
TiO_2 nanofibers	220.7/0.04	-	155/0.04/100	29
Hollow TiO_2 nanostructures	280/0.173	140.8/1.73	199.5/0.173/60 127.7/1.73/1000	30
Mesoporous TiO_2 spheres	256.3/0.1675	113.4/3.35	196.0/0.1675/100 110.2/3.35/3000	31
TiO_2(B) nanosheet-assembled hierarchical tubes	290/0.335	202/0.67 182/1.675 160/3.35 130/6.7	160/1.675/400	32
Hollow TiO_2 microboxes	205/0.17	63/3.4	187/0.17/300	33
Mesoporous TiO_2 nanowire bundles	293/0.0334	199/0.0835 175/0.167 162/0.334 134/0.835 112/1.67	174/0.167/100 96/8.35/50	34
TiO_2 hollow spheres	187.4/0.173	145.2/0.173 127.3/0.346 120.1/0.865 105.6/1.73 81.4/3.46 60.8/6.92	147.6/0.173/300	35
Multishelled TiO_2 hollow microspheres	260/0.1675	129/1.675	237/0.1675/100 119/1.675/1200	36

References

1. J. U. Ha, J. Lee, M. A. Abbas, M. D. Lee, J. Lee and J. H. Bang, *ACS Appl. Mater. Interfaces*, 2019, **11**, 11391-11402.
2. P. Niu, T. Wu, L. Wen, J. Tan, Y. Yang, S. Zheng, Y. Liang, F. Li, J. T. S. Irvine, G. Liu, X. Ma and H.-M. Cheng, *Adv. Mater.*, 2018, **30**, 1705999.
3. M. Luo, X. Yu, W. Zhao, R. Xu, Y. Liu and H. Shen, *ACS Appl. Mater. Interfaces*, 2018, **10**, 35060-35068.
4. H. Zhu, Y. Jing, M. Pal, Y. Liu, Y. Liu, J. Wang, F. Zhang and D. Zhao, *Nanoscale*, 2017, **9**, 1539-1546.
5. Y. Wang, S. Duan, Z. Tian, Y. Shen, M. Xie, X. Guo and X. Guo, *J. Mater. Chem. A*, 2017, **5**, 6047-6051.
6. Y. Liu, A. A. Elzatahry, W. Luo, K. Lan, P. Zhang, J. Fan, Y. Wei, C. Wang, Y. Deng, G. Zheng, F. Zhang, Y. Tang, L. Mai and D. Zhao, *Nano Energy*, 2016, **25**, 80-90.
7. S. Chu, Y. Zhong, R. Cai, Z. Zhang, S. Wei and Z. Shao, *Small*, 2016, **12**, 6724-6734.
8. R. Wu, S. Shen, G. Xia, F. Zhu, C. Lastoskie and J. Zhang, *ACS Appl. Mater. Interfaces*, 2016, **8**, 19968-19978.
9. H.-B. Huang, Y. Yang, L.-H. Chen, Y. Wang, S.-Z. Huang, J.-W. Tao, X.-T. Ma, T. Hasan, Y. Li, Y. Xu and B.-L. Su, *Nanoscale*, 2016, **8**, 10928-10937.
10. H. Liu, W. Li, D. Shen, D. Zhao and G. Wang, *J. Am. Chem. Soc.*, 2015, **137**, 13161-13166.
11. W. Cheng, F. Rechberger, D. Primc and M. Niederberger, *Nanoscale*, 2015, **7**, 13898-13906.
12. C. Zhang, Q. Zhang, S. Kang and X. Li, *J. Mater. Chem. A*, 2014, **2**, 2801-2806.
13. L. Pan, Z.-W. Zhou, Y.-T. Liu and X.-M. Xie, *J. Mater. Chem. A*, 2018, **6**, 7070-7079.
14. W. Zhang, T. Xu, Z. Liu, N.-L. Wu and M. Wei, *Chem. Commun.*, 2018, **54**, 1413-1416.
15. A. Mondal, S. Maiti, K. Singha, S. Mahanty and A. B. Panda, *J. Mater. Chem. A*, 2017, **5**, 23853-23862.
16. Y. Cheng, Z. Chen, H. Wu, M. Zhu and Y. Lu, *Adv. Funct. Mater.*, 2016, **26**, 1338-1346.
17. W. Li, F. Wang, Y. Liu, J. Wang, J. Yang, L. Zhang, A. A. Elzatahry, D. Al-Dahyan, Y. Xia and D. Zhao, *Nano Lett.*, 2015, **15**, 2186-2193.
18. Z. Zhang, L. Zhang, W. Li, A. Yu and P. Wu, *ACS Appl. Mater. Interfaces*, 2015, **7**, 10395-10400.
19. B. Qiu, M. Xing and J. Zhang, *J. Am. Chem. Soc.*, 2014, **136**, 5852-5855.
20. R. Mo, Z. Lei, K. Sun and D. Rooney, *Adv. Mater.*, 2014, **26**, 2084-2088.
21. X. Jiang, X. Yang, Y. Zhu, H. Jiang, Y. Yao, P. Zhao and C. Li, *J. Mater. Chem. A*, 2014, **2**, 11124-11133.
22. Z. Wang, J. Sha, E. Liu, C. He, C. Shi, J. Li and N. Zhao, *J. Mater. Chem. A*, 2014, **2**, 8893-8901.
23. W. Li, F. Wang, S. Feng, J. Wang, Z. Sun, B. Li, Y. Li, J. Yang, A. A. Elzatahry, Y. Xia and D. Zhao, *J. Am. Chem. Soc.*, 2013, **135**, 18300-18303.
24. X. Xin, X. Zhou, J. Wu, X. Yao and Z. Liu, *ACS Nano*, 2012, **6**, 11035-11043.
25. H. Ren, R. Yu, J. Qi, L. Zhang, Q. Jin and D. Wang, *Adv. Mater.*, 2019, **31**, 1805754.
26. D.-H. Lee, B.-H. Lee, A. K. Sinha, J.-H. Park, M.-S. Kim, J. Park, H. Shin, K.-S. Lee, Y.-E. Sung and T. Hyeon, *J. Am. Chem. Soc.*, 2018, **140**, 16676-16684.
27. H. Wei, E. F. Rodriguez, A. F. Hollenkamp, A. I. Bhatt, D. Chen and R. A. Caruso, *Adv. Funct. Mater.*, 2017, **27**, 1703270.
28. Y. Li, S. Wang, Y.-B. He, L. Tang, Y. V. Kaneti, W. Lv, Z. Lin, B. Li, Q.-H. Yang and F. Kang, *J. Mater. Chem. A*, 2017, **5**, 4359-4367.
29. S. Lee, W. Eom, H. Park and T. H. Han, *ACS Appl. Mater. Interfaces*, 2017, **9**, 25332-25338.
30. B. Y. Guan, L. Yu, J. Li and X. W. Lou, *Sci. Adv.*, 2016, **2**, e1501554.
31. H. Ren, J. Sun, R. Yu, M. Yang, L. Gu, P. Liu, H. Zhao, D. Kisailus and D. Wang, *Chem. Sci.*, 2016, **7**, 793-

798.
32. H. Hu, L. Yu, X. Gao, Z. Lin and X. W. Lou, *Energy Environ. Sci.*, 2015, **8**, 1480-1483.
33. X. Gao, G. Li, Y. Xu, Z. Hong, C. Liang and Z. Lin, *Angew. Chem. Int. Ed.*, 2015, **54**, 14331-14335.
34. J. Jin, S.-Z. Huang, J. Liu, Y. Li, L.-H. Chen, Y. Yu, H.-E. Wang, C. P. Grey and B.-L. Su, *Adv. Sci.*, 2015, **2**, 1500070.
35. G. Zhang, H. B. Wu, T. Song, U. Paik and X. W. Lou, *Angew. Chem. Int. Ed.*, 2014, **53**, 12590-12593.
36. H. Ren, R. Yu, J. Wang, Q. Jin, M. Yang, D. Mao, D. Kisailus, H. Zhao and D. Wang, *Nano Lett.*, 2014, **14**, 6679-6684.